HOKKAIDO UNIVERSITY

Title	Tsunami hazard in the Caribbean coast of Honduras due to large earthquakes occurred along the Cayman Trough at the northwest boundary of Caribbean plate
Author(s)	Tanioka, Yuichiro; Cabrera, Amilcar Geovanny; Arguello, Greyving Jose et al.
Citation	Coastal Engineering Journal, 62(3), 405-412 https://doi.org/10.1080/21664250.2020.1744061
Issue Date	2020
Doc URL	https://hdl.handle.net/2115/84234
Rights	This is an Accepted Manuscript of an article published by Taylor & Francis in Coastal engineering journal on 2020, available online: http://www.tandfonline.com/https://doi.org/10.1080/21664250.2020.1744061.
Type	journal article
File Information	Coastal Eng J_2020.pdf

1 **Tsunami hazard in Caribbean Coast of Honduras due to Large Earthquakes**

2 **Occurred along the Cayman Trough at the Northwest boundary of Caribbean plate.**

3

4 Yuichiro Tanioka[1], Amilcar Geovanny Cabrera[2], Greyving Jose Arguello[2],

5 and Yusuke Yamanaka[3]

6

7 1) Institute of Seismology and Volcanology, Faculty of Science, Hokkaido University,

8   N10W8, Kita-ku, Sapporo, Japan, 060-0810

9 2) Nicaraguan Institute of Territorial Studies, Managua, Nicaragua.

10 3) Department of Civil Engineering, The University of Tokyo, Tokyo 113-8656, Japan

11

12

13 (Revised parts are shown in red.)

14

15

16

17

18

19

20

21

22

23

24

25

26

28 **Abstract**

29 In 2018, a large earthquake (Mw7.6) occurred in the Swan Island Fault zone at the northwest

30 boundary of the Caribbean plate. This earthquake generated only a small tsunami of 20 cm.

31 However, Puerto Cortes in Honduras is located close to the Swan Island Fault zone. Evaluation

32 of tsunami hazard at Puerto Cortes due to large earthquakes along the fault zone is important. We

33 first estimated the fault parameters of the 2018 Swan Island earthquake using W-phase inversion

34 technique. Then, the moment magnitude of 7.6, the fault length of 134 km, the fault width of 24

35 km, and the slip amount of 5.1 m were estimated. In addition to those estimates, a small fault

36 dimension of the earthquake, 40 km × 20 km, with a slip amount of 20.8 m was considered. Those

37 two fault models were used to compute tsunami inundation at Puerto Cortes. The tsunami

38 computed from the small fault inundated a large area in Puerto Cortes including the port area. The

39 effect of co-seismic horizontal displacement of ocean floor also enhanced the tsunami inundation

40 there. Those results indicate that preparation for future tsunami hazard in Puerto Cortes is

41 important although no significant tsunami was generated historically.

42

43 **Key words:** Tsunami hazard; Puerto Cortes in Honduras; The 2018 Swan Island earthquake.

44

45 **1. Introduction**

46

47   On 9th of January in 2018, a large earthquake (Mw7.6) occurred in the Swan Island Fault zone

48 at the northwestern boundary of the Caribbean plate (Figure 1). The location and mechanism of

49 the earthquake from the Global CMT catalog show a left-lateral strike-slip fault motion along the

50 Swan Island fault zone. The tsunami warning was issued from the Pacific Tsunami Warning

51 Center immediately after the earthquake. Only small tsunami was generated by the earthquake

52 and was observed at George Town in Cayman Islands, United Kingdom. The observed amplitude

53 of the tsunami was about 20 cm.

54   The 2010 large Haiti earthquake (Mw7.0) generated tsunamis along the coast of Haiti in

55 Caribbean Sea (Fritz et al., 2013). Historically, several large earthquakes have occurred along the

56 Swan Island fault zone (Figure 1). In 1976, the Guatemala large earthquake (Ms7.5) occurred

57 along the Motagua fault which is located at the western end of the Swan Island fault zone (Plafker,

58 1977). The surface rupture was extended about 230 km with a left-lateral displacement. The

59 strong shaking caused more than 23,000 casualties, the most destructive earthquake in Guatemala

60 since 1917. Because the earthquake occurred inland, the tsunami was not generated. In 1999, the

61 Guatemala earthquake (Mw 6.7) occurred beneath the Caribbean coast of Guatemala with a left-

62 lateral fault motion. The strong motion caused one casualty and destroyed several houses in

63 Guatemala. In 2009, the off-Honduras earthquake (Mw7.3) occurred along the Swan Island fault

64 zone in Gulf of Honduras (Figure 1). The strong shaking in northern Honduras caused 7 casualties

65 and destroyed 130 buildings (https://earthquake.usgs.gov/earthquakes/eventpage/usp000gxkj/

66 impact).

67   Although there were no damages reported by tsunamis generated by those historical large

68 earthquakes, the concern of tsunami risk along the northern coast of Honduras has been increased

69 after the 2018 large Swan Island earthquake. Especially, evaluation of the tsunami risk at Puerto

70 Cortes in Honduras, one of the largest seaports in Central America, is an important issue because

71 Puerto Cortes is located very close to the Swan Island fault zone (Figure 1). Also, in 2016, the

72 Central American Tsunami Advisory Center (CATAC) was started to establish at the Nicaraguan

73 Institute of Territorial Studies with Japanese cooperation (Strauch et al., 2018). This center should

74 be completed in 2019. Evaluation of tsunami hazard along the coast in Central America is also

75 one of important tasks in the CATAC.

76   In this study, at first, the source model of the 2018 large Swan Island earthquake is determined

77 by using the W-phase inversion (Kanamori and Rivera, 2008) and the scaling relationship (Blaser

3

78   et al., 2010). Then, the tsunami hazard at Puerto Cortes in the northern coast of Honduras is

79   evaluated from realistic fault models based on the fault models of the 2018 large Swan Island

80   earthquake. Finally, the tsunami risk at Puerto Cortes in Honduras is discussed.

81

82   **2. Data**

83

84   Low-frequency broadband seismic records from the database at the German Research Center

85   for Geosciences (GRCG or GFZ) catalog were downloaded. The vertical components of 49

86   stations located at epicentral distance less than 90 degrees are used for the W-phase inversion.

87   The General Bathymetry Chart of the Oceans (GEBCO) dataset of 30 arcseconds grid spacing,

88   the nautical chart (#28170) of Puerto Cortes (Gulf of Honduras), and the topography data, Shuttle

89   Radar Topography Mission (SRTM) with a resolution of 1 arcseconds, are used for the tsunami

90   inundation simulation.

91

92   **3. Method**

93

94   *3.1 Estimation of Fault model*

95   The W phase, a distinct long-period (100–1000 s) phase arrives before the S phase and can be

96   used for rapid and robust determination of great earthquake source parameters (Kanamori and

97   Rivera 2008; Duputel et al. 2011). This W-phase inversion algorithm is used to estimate the

98   magnitudes, the centroid locations, and the mechanisms of the 2018 Swan Island earthquake

99   (Mw7.6). Time domain deconvolution is used to retrieve displacement waveforms from the

100   broadband seismograms. Then, they are bandpass filtered between 0.00167 and 0.005 Hz using

101   fourth order of Butterworth filter. The time window (in seconds) used in the inversion is set

102   between P wave arrival and that plus 15 times the distance (degree) between the epicenter and the

103   station.

104   Scaling relationships are used to estimate the length and width of the fault model from the

105   estimated moment magnitude by the W-phase inversion. Blaser et al. (2010) determined the

106   empirical relationship between the fault length, L (km), and moment magnitude, Mw, as shown

107   in Equation (1), and the relationship between the fault width, W (km), and moment magnitude,

108   Mw, as shown in Equation (2) for large oceanic strike-slip earthquakes in the world.

109 $$\log L = -2.56 + 0.62 Mw \tag{1}$$

110 $$\log W = -0.66 + 0.27 Mw \tag{2}$$

111   A slip amount, D (m), is calculated from Equation (3):

112 $$D = \frac{M_0}{\mu L W} \text{ , where } M_0 = 10^{1.5 M_w + 9.1} \tag{3}$$

113   where M_0 (Nm) is the seismic moment, L is the fault length in m, W is the fault width in m, and

114   μ is a rigidity that is assumed to be $1.7 \times 10^{10} \, N/m^2$, which is the smallest for shallow

115   earthquakes in the crust. The center of the fault is located at the centroid of the W-phase inversion.

116

117   *3.2. Tsunami Numerical Simulation*

118   The vertical ocean bottom deformation due to an earthquake is computed from the fault model

119   using the equations of Okada (1985). Then, the vertical ocean surface deformation due to the co-

120   seismic horizontal displacement of ocean bottom (Tanioka and Satake, 2006) is added to the co-

121   seismic vertical deformation. This vertical deformation is used as the tsunami initial surface

122   deformation. The tsunami propagation is numerically computed using the non-linear shallow

123   water equations solved by the finite difference scheme (Goto et al. 1997). Tsunami inundation is

124   numerically computed using a moving boundary condition (Imamura 1996). A Manning's

125   roughness coefficient in the non-linear shallow water equations is assumed to be 0.025 sm$^{-1/3}$.

126   Four nested grid systems are used for this tsunami simulation (Figure 2). For Region 1 (R1), the

127   bathymetry GEBCO 30 arcseconds was resampled to make 27 arcseconds grid system. For

128   Regions 2 and 3 (R2 and R3), it was interpolated to make 9 and 3 arcseconds grid systems,

129   respectively. For Region 4 (R4), the nautical cart (#28170) for Puerto Cortes was digitized and

130   combined with Shuttle Radar Topography Mission (SRTM) 1 arcsecond topography data to make

131   1 arcsecond grid system. Finally, the 1 arcsecond topography data along the coast of Puerto Corte

132   are manually corrected using the topography map (Figure 3).

133

134   **4. Result**

135

136   *4.1. Fault model for the 2018 Swan Island earthquake*

137   The solution of W-phase inversion gives a seismic moment of 2.85 x 10^{20} Nm (Mw 7.57), a

138   left-lateral strike-slip mechanism (strike = 254.4°, dip = 66.8°, rake = -11.1°), a centroid location

139   (longitude 83.75°W, latitude 17.46°N), a centroid depth of 11.5 km (Figure 4). The fault length

140   and width estimated from the scaling relationships, equation (1) and (2), (Blaser et al., 2010) are

141   134 km and 24 km, respectively. The slip amount is calculated to be 5.1 m using equation (3).

142   The estimated slip distribution of the 2018 Swan Island earthquake was shown in the USGS

143   earthquake catalog (https://earthquake.usgs.gov/earthquakes/eventpage/us1000c2zy/finite-fault).

144   This indicated that the slip was more concentrated near the epicenter, the fault length of about 40

145   km and the fault width of about 20 km. This may indicate that the world-wide scaling relationships

146   do not work for large earthquakes in this fault zone. Therefore, we decided to use this small fault

147   area of 40 km x 20 km for one of fault models to evaluate tsunami hazard at Puerto Cortes in

148   Honduras. The slip amount for the small fault is calculated to be 20.8 m.

149

150   *4.2. Tsunami inundation simulation at Puerto Cortes*

151   A long fault model of 136 km x 24 km using the scaling relationships and a small fault model

152   of 40 km x 20 km based on the slip distribution of the 2018 earthquake are used to compute

153   tsunami inundation at Puerto Cortes in Figure 3. We located these fault models off Puerto Cortes

154   along the Swan Island fault zone (Figure 4). The mechanism and the seismic moment are the same

155   as the 2018 Swan Island earthquake. The co-seismic horizonal displacement of the ocean bottom

156 (Tanioka and Satake, 1996) should be important for the tsunami generation because of the strike-

157 slip type of the fault models. Therefore, four tsunami inundations at Puerto Cortes are numerically

158 computed using two fault models with the tsunami generation due to the horizontal displacement

159 or without that.

160   In Figure 5, the tsunami initial conditions from the long fault model with the effect of the

161 horizontal displacement and without that are compared. In Figure 6, the tsunami inundations at

162 Puerto Cortes computed from those two initial conditions are compared. The tsunami numerical

163 simulations from both initial conditions cause limited inundations and do not cause serious

164 damages in the port area although the tsunami heights from the tsunami initial condition with the

165 effect of the horizonal displacement are larger than those from the tsunami initial condition

166 without the effect.

167   In Figure 7, the tsunami initial conditions from the small fault model with the effect of the

168 horizontal displacement and without that are compared. In Figure 8, the tsunami inundations at

169 Puerto Cortes computed from those two initial conditions are compared. The western part of the

170 beach and city are inundated by tsunamis of about 4 m maximum height from both initial

171 conditions. The port area is also inundated by the tsunami. The inundation area computed from

172 the initial condition with the effect of the horizontal displacement is slightly larger than that from

173 the initial condition without that. Especially, at the port area, shown as a red ellipse in Figure 8,

174 the tsunami inundation is larger for the tsunami initial condition with the horizontal displacement

175 effect than that for the initial condition without the effect. Figure 9 shows the comparison of two

176 computed tsunami waveforms with and without the effect of horizonal displacement. The

177 maximum tsunami height from the initial condition with the horizontal displacement effect is

178 14 % larger than that from the initial condition without the effect.

179

180 **5. Discussions**

181   Because the 2018 large Swan Island earthquake (Mw 7.6) occurred far from the coast of Central

182 America (Figure 1), only small tsunami, less than 20 cm, was observed. The results in this study

183 show that the same size of earthquake occurred near Puerto Cortes along the left-lateral Swan

184 Island Fault zone cause significant tsunami inundation which could damage one of the largest

185 ports in Central America and the residents. Large cargo boats in the port can be damaged easily

186 by those tsunamis. Large cargo boats carried by the tsunamis also damage the port and residents.

187 It is important to understand this possible tsunami hazard and prepare for that.

188   The horizontal displacement of ocean bottom slops near the Swan Island Fault zone in this area

189 enhanced the tsunami generation as shown in Figure 7. In general, strike-slip type earthquakes

190 cause much larger horizontal displacement than vertical displacement. This causes that the

191 enhancement of tsunami generation due to the horizontal displacement of the ocean slops by

192 strike-slip type earthquakes is more significant than that the enhancement by the dip-slip

193 earthquakes. Figure 9 indicates that the enhancement in this study reaches about 14% of the

194 tsunami height without the horizontal displacement effect.

195

196 **6. Conclusions**

197

198   The tsunami inundation at Puerto Cortes was computed from two fault models in the Swan Island

199 Fault zone, the long fault model estimated from the scaling relationships (Blaser et al., 2010) and

200 the small fault model estimated from the slip distribution based on the 2018 Swan Island

201 earthquake. The tsunami computed from the small fault model with a large slip amount of 20.8 m

202 inundated a large area of Puerto Cortes including the important port area. Large cargo boats in the

203 port can be damaged easily by those tsunamis. The effect of the co-seismic horizontal

204 displacement of the ocean floor also enhanced the tsunami inundation at Puerto Cortes.

205   The Swan Island Fault zone accommodates the relative motion between the North American and

206 Caribbean plates, 2 cm/yr (Dixon et al., 1998, ten Brink et al, 2002, Mann, 2007). Consequently,

207 the large earthquakes repeatedly occurred along the Swan Island fault zone, such as the 1976

208 Guatemala earthquake (Ms 7.5), the 1999 Guatemala earthquake (Mw6.7), the 2009 Off Honduras

209 earthquake (Mw 7.3), and the 2018 Swan Island earthquake (Mw 7.6). However, no large

210 earthquake (Ms > 7) occurred off Puerto Cortes along the fault zone at least 50 years. We need to

211 prepare for a large future earthquake off Puerto Cortes and tsunami hazard at Puerto Cortes.

212

217

218

219 **References**

220 Blaser, L., Kru¨ger, F., Ohrnberger, M., and Scherbaum, F., (2010). Scaling relations of earthquake

221   source parameter estimates with special focus on subduction environment. Bulletin of the

222   Seismological Society of America, 100(6), 2914–2926. doi:10.1785/0120100111.

223 Dixon, T. H., Farina, F., DeMets, C., Jansma, P. E., Mann, P., and Calais, E. (1998). Relative

224   motion between the Caribbean and North American plates and related boundary zone

225   deformation from a decade of GPS observations. Journal of Geophysical Research, 103,

226   15157–15182.

227 Duputel, Z., Rivera, L., Kanamori, H., and Hayes, G. (2011). Realtime W phase inversion during

228   the 2011 off the Pacific coast of Tohoku earthquake. Earth Planets Space, 63, 535–539.

229   doi:10.5047/eps.2011.05.032.

230 Fritz, H.M., J.V. Hillaire, E. Molière, Y. Wei, and F. Mohammed (2013). Twin tsunamis triggered

231   by the 12 January 2010 Haiti earthquake. Pure Appl. Geophys., 170(9-10):1463-1474,

232   doi:10.1007/s00024-012-0479-3.

233 Goto, C., Ogawa, Y., Shuto, N., and Imamura, F., (1997). IUGG/IOC time project: Numerical

234   method of tsunami simulation with the leap-flog scheme, IOC of UNESCO, manuals and

235   guides 35.

236   Imamura, F. (1996). Review of tsunami simulation with a finite difference method. In H. Yeh, P.

237   Liu, and C. Synolakis (Eds.), Long-Wave Runup Models (pp. 25–42). World Scientific.

238   Kanamori, H., & Rivera, L. (2008). Source inversion of W phase: speeding up seismic tsunami

239   warning. Geophysical Journal International, 175(1), 222–238.

240   Mann, P., (2007), Overview of the tectonic history of northern Central America, *in* Mann, P.,

241   ed., Geologic and tectonic development of the Caribbean plate boundary in northern Central

242   America: Geological Society of America Special Paper 428, 1–19,

243   doi:10.1130/2007.2428(01).

244   Okada, Y., (1985), Surface deformation due to shear and tensile faults in a half-space. Bulletin of

245   the Seismological Society of America, 75, 1135–1154.

246   Plafker, G., (1977), Color slides showing geologic effects and damage caused by the destructive

247   Guatemala earthquake of February 4, 1976, United State Department of the Interior,

248   Geological Survey Open-file Report 77-165, 1-10.

249   Strauch, W., Talavera E., Tenorio V., Ramirez J., Arguello G., Herrera M., Acosta A., and

250   Morales A., (2018), Toward an Earthquake and Tsunami Monitoring and Early Warning

251   System for Nicaragua and Central America, Seismological Research Letters, 89, 400-406,

252   doi: 10.1785/0220170193.

253   Tanioka, Y., and Satake, K. (1996), Tsunami generation by horizontal displacement of ocean

254   bottom. Geophysical Research Letters, 23(8), 861-864

255   ten Brink, U.S., Coleman, D.F., and Dillon, W.P. (2002), The nature of the crust under Cayman

256   trough from gravity: Marine and Petroleum Geology, 19, 971–987, doi: 10.1016/S0264-

257   8172(02)00132-0.

258

259   **Figure Captions**

260

261 Figure 1. Large earthquakes occurred along the Swan Island Fault Zone, the 1976 Guatemala

262 earthquake (Ms7.5), the 1999 Guatemala earthquake (Mw 6.7), the 2009 Off-Honduras

263 earthquake (Mw7.3), and the 2018 Swan Inland earthquake (Mw7.6). The red line shows the

264 Swan Island Fault Zone (after ten Brink et al., 2002).

265

266 Figure 2. Four nested grid systems (R1, R2, R3, and R4) for the tsunami numerical simulation.

267 Tsunami inundation simulation is carried out for R4 region at Puerto Cortes. The red line shows

268 the Swan Island Fault Zone (after ten Brink et al., 2002).

269

270 Figure 3. Bathymetry and topography in R4 region (Puerto Cortes) where tsunami inundation

271 simulation is carried out.

272

273 Figure 4. The focal mechanism and fault model (a black rectangular) of the 2018 Swan Island

274 earthquake estimated using the W-phase inversion and the scaling relationships between

275 magnitude and the fault length or width (Blaser et al., 2010). Purple rectangles show two fault

276 models, 136 km x 24 km, and 40 km, x 20 km, for the tsunami hazard evaluation at Puerto

277 Cortes. The red line shows the Swan Island Fault Zone (after ten Brink et al., 2002).

278

279 Figure 5. Tsunami initial sea surface deformation for the long fault model (136 km x 24 km) from

280 the scaling relationships (Blaser at al., 2010). a) no effect of the co-seismic horizontal

281 displacement. b) including the effect of the co-seismic horizontal displacement.

282

283 Figure 6. The results of the tsunami inundation at Puerto Cortes computed from the initial sea

284 surface deformation in Figure 5 using the long fault model. a) no effect of the co-seismic

285 horizontal displacement. b) including the effect of the co-seismic horizontal displacement.

11

286

287   Figure 7. Tsunami initial sea surface deformation for the small fault model (40 km x 20 km) based

288   on the slip distribution estimated by the USGS. a) no effect of the co-seismic horizontal

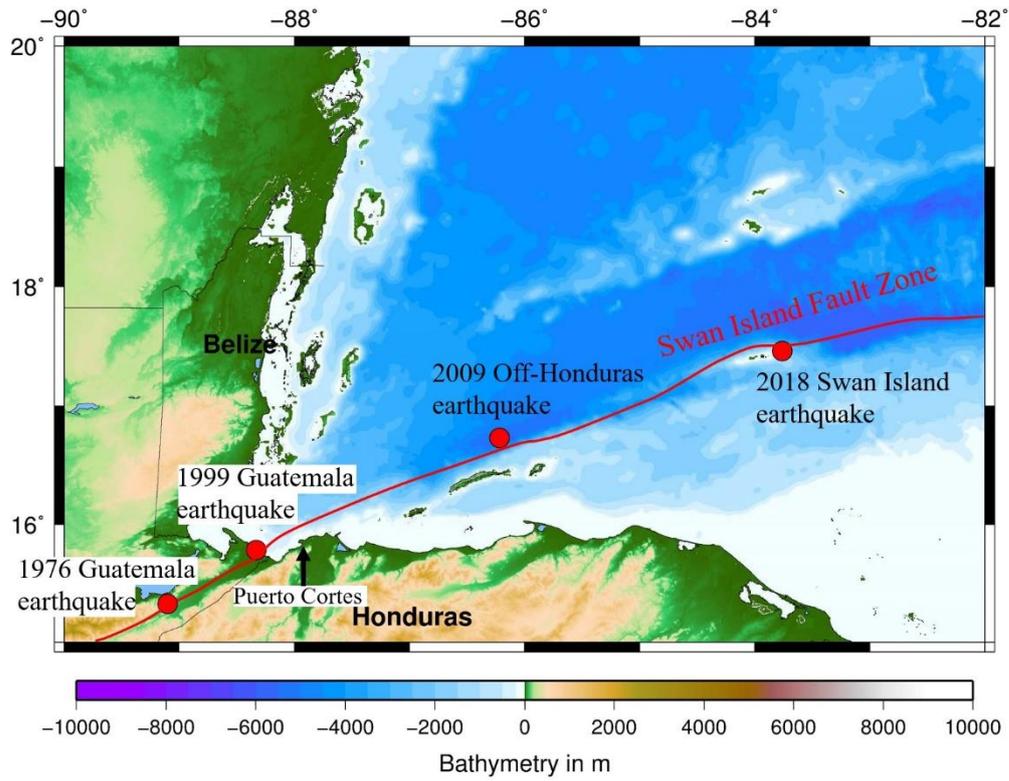289   displacement. b) including the effect of the co-seismic horizontal displacement.

290

291   Figure 8. The results of the tsunami inundation at Puerto Cortes computed from the initial sea

292   surface deformation in Figure 7 using the small fault model. a) no effect of the co-seismic

293   horizontal displacement. b) including the effect of the co-seismic horizontal displacement. Red

294   ellipse shows the port area. A black dot shows a location of tsunami waveform comparison in

295   Figure 9.

296

297   Figure 9. Comparison of tsunami waveforms at a position, P, in Figure 8 for the initial condition

298   with horizontal displacement effect (blue) and for that without the effect (red).
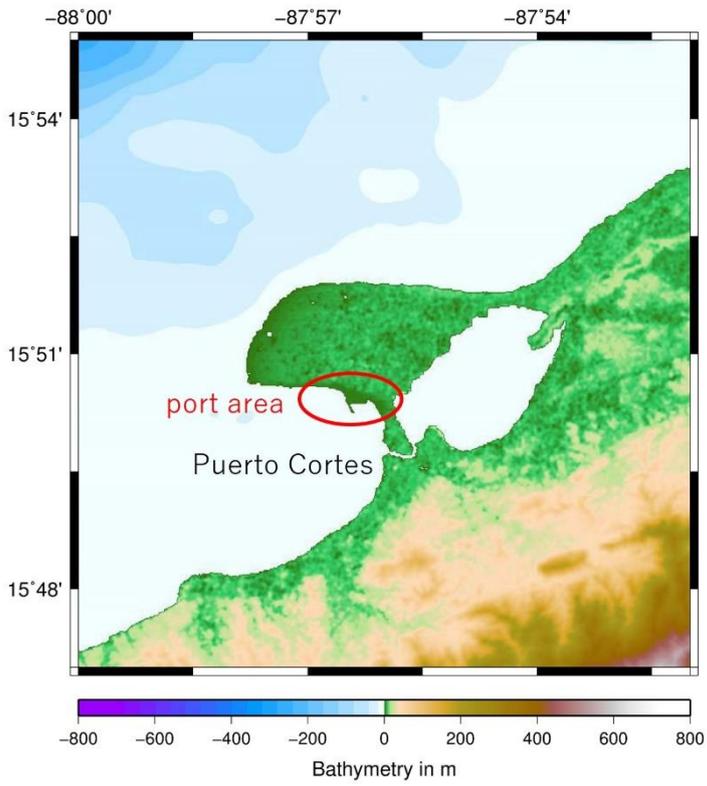
299

300

301

302   Figure 1.

303
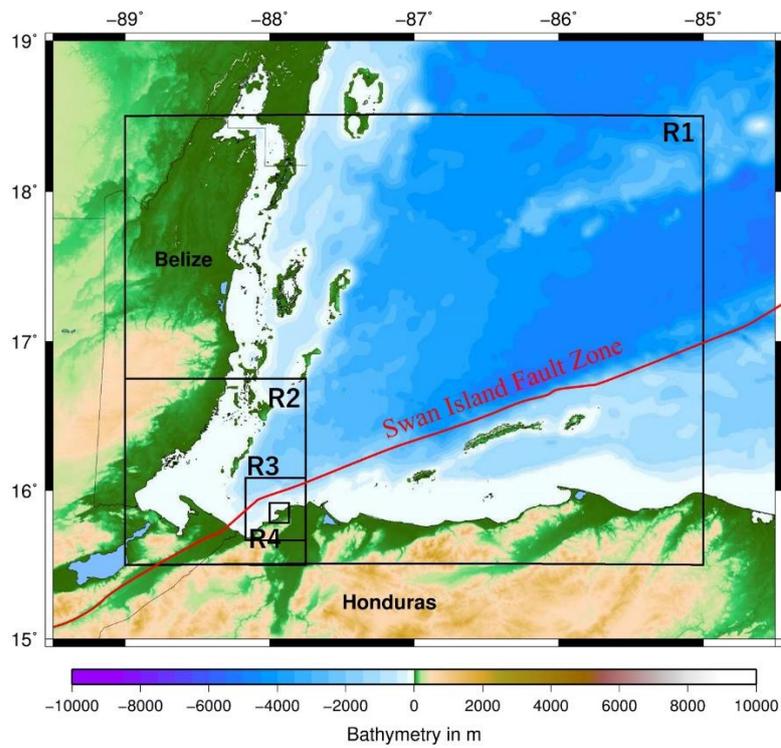
304

305   Figure 2.

306

Figure 3.

308

Figure 4.

310

311

a) No horizontal displacement effect
b) Horizontal displacement effect

312 Figure 5.

313

a) No horizontal displacement effect
b) Horizontal displacement effect

314 Figure 6.

315

a) No horizontal displacement effect
b) Horizontal displacement effect

316 Figure 7.

15

a) No horizontal displacement effect

b) Horizontal displacement effect
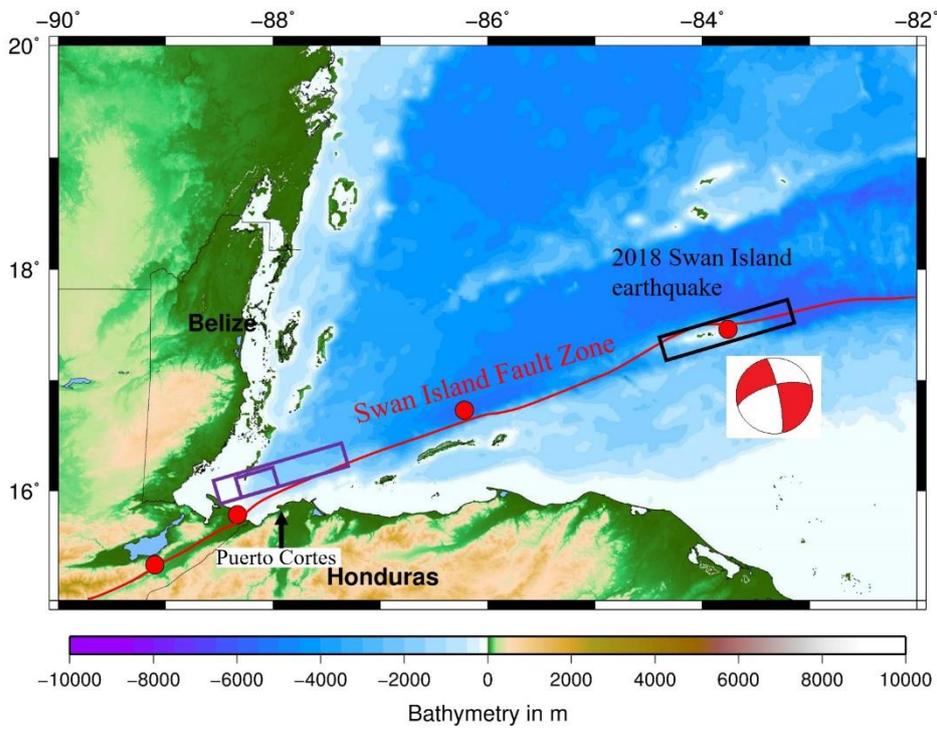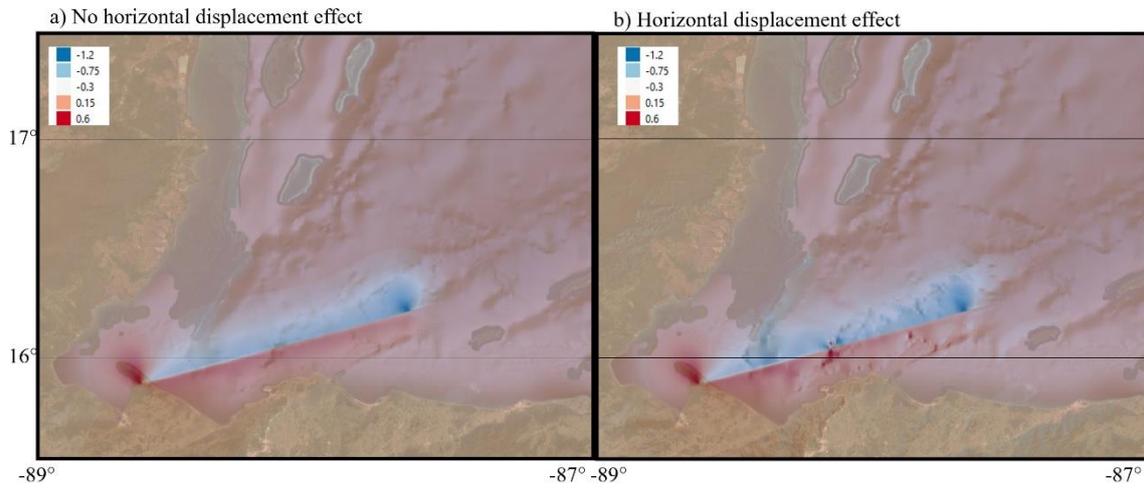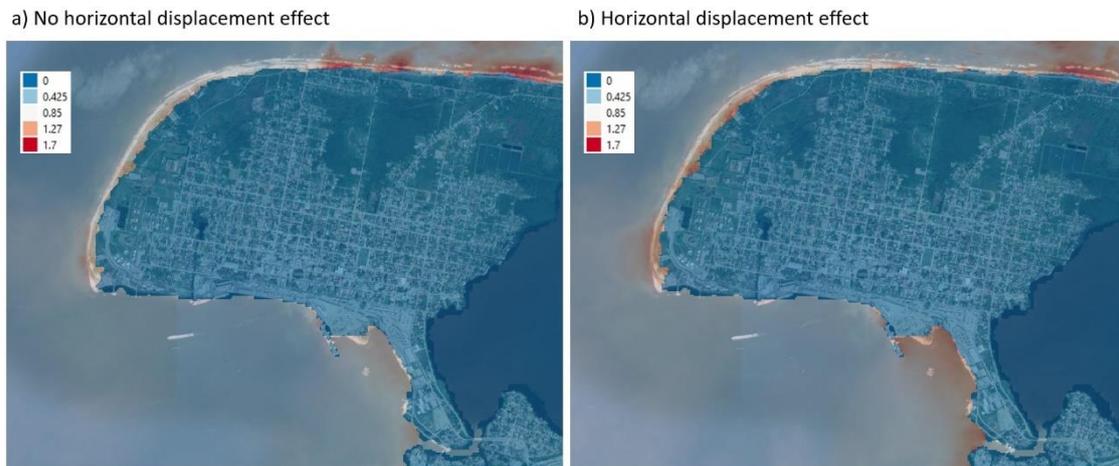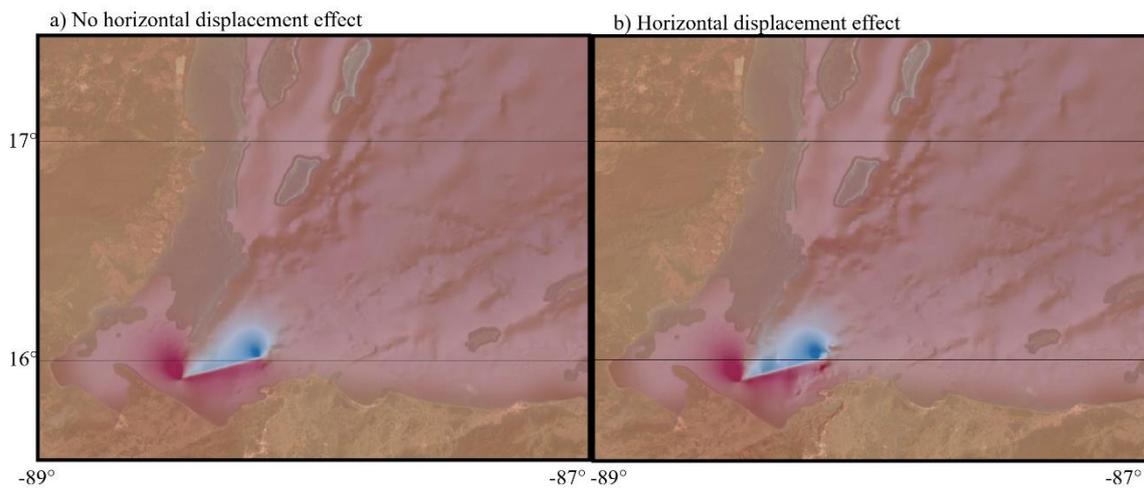
317

318   Figure 8.

319

320

321   Figure 9